EFFICIENT MODELING OF ELECTROMAGNETIC SCATTERING BY SYMMETRIC LAMELLAR PERIODIC STRUCTURES AT NORMAL INCIDENCE

K. M. Leung*
Polytechnic University, Department of Computer and Information Science,
Six Metrotech Center, Brooklyn, NY 11201

T. Tamir
Polytechnic University, Department of Electrical and Computer Engineering
Six Metrotech Center, Brooklyn, NY 11201

ABSTRACT

An efficient modeling of the electromagnetic scattering properties of symmetric lamellar periodic structures at normal incidence is discussed within the framework of the modal-field approach. By taking advantage of the inherent symmetry, a numerical computational speedup of up to 8 times can be achieved by explicitly ignoring anti-symmetric modes, which play no role in the scattering process at all.

1 INTRODUCTION

We consider here the special problem of electromagnetic scattering of normal incident waves onto a lamellar periodic structure whose unit cell possesses a plane about which the structure exhibits a reflection symmetry. This problem is commonly encountered in corrugated quantum well infrared photodetectors (C-QWIPs). (Choi 1997, Mao et al. 2002, Choi et al. 2003, 2004a,b,c) Other applications include anti-reflection coatings and interference filters.

QWIPs have applications in many different areas, including industrial, medical, geological, environmental, homeland security, and defense. In the case of defense, they are critical to all phases of any ballistic missile system, including missile seeking and detection, and decoy countermeasure. They also have applications in long range surveillance and land-mine detection

An example of a symmetric C-QWIP structure is shown in Fig. 1. The structure has a semi-infinite substrate below and a semi-infinite cover region at the top, with 3 grating layers sandwiched between them. These grating layers consist of a multiple quantum-well (MQW) layer of thickness t_q sandwiched between two semi-conductor layers of thicknesses t_c and t_b. The MQW region is assumed to have a biaxial dielectric constant given by ϵ^y in the vertical direction and by ϵ^x in the horizontal direction. The width for the air region is s, and that for the MQW region is w, and so the lattice spacing a is $s + w$. The incident wave is assumed to be a plane TM polarized wave incident from below and traveling perpendicularly to the layers.

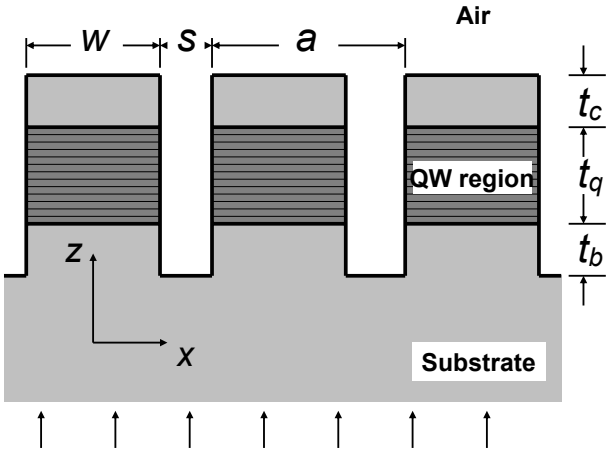

Figure 1: An example of a C-QWIP structure.

Modeling and optimizing the performance of photodetectors like the present one presents certain challenges. First of all there must be strong diffraction of the waves within the structure. This means that the various dimensions of the structure must be comparable to the wavelength of the incident radiation, and the dielectric contrast must also be sufficiently strong. Modeling of diffraction in such a strongly scattering medium is known to be always challenging and requires accurate handling of the entire set of Maxwell's equations with its associated set of boundary conditions.

Secondly, photodetector structures are intrinsically multilayered. The above simple example of a C-QWIP consists of only 5 layers (3 periodic layers and 2 semi-infinite homogeneous layers). More realistic devices often have metallic layers and other dielectric layers for various electrical and mechanical and structural purposes. The number of layers quickly increases when

Report Documentation Page

Form Approved
OMB No. 0704-0188

1. REPORT DATE	2. REPORT TYPE	3. DATES COVERED
00 DEC 2004	**N/A**	**-**

4. TITLE AND SUBTITLE	5a. CONTRACT NUMBER
Efficient Modeling Of Electromagnetic Scattering By Symmetric Lamellar Periodic Structures At Normal Incidence	5b. GRANT NUMBER
	5c. PROGRAM ELEMENT NUMBER
6. AUTHOR(S)	5d. PROJECT NUMBER
	5e. TASK NUMBER
	5f. WORK UNIT NUMBER
7. PERFORMING ORGANIZATION NAME(S) AND ADDRESS(ES) **Polytechnic University, Department of Computer and Information Science, Six Metrotech Center, Brooklyn, NY 11201; Polytechnic University, Department of Electrical and Computer Engineering Six Metrotech Center, Brooklyn, NY 11201**	8. PERFORMING ORGANIZATION REPORT NUMBER
9. SPONSORING/MONITORING AGENCY NAME(S) AND ADDRESS(ES)	10. SPONSOR/MONITOR'S ACRONYM(S)
	11. SPONSOR/MONITOR'S REPORT NUMBER(S)

12. DISTRIBUTION/AVAILABILITY STATEMENT
Approved for public release, distribution unlimited

13. SUPPLEMENTARY NOTES
See also ADM001736, Proceedings for the Army Science Conference (24th) Held on 29 November - 2 December 2005 in Orlando, Florida. , The original document contains color images.

14. ABSTRACT

15. SUBJECT TERMS

16. SECURITY CLASSIFICATION OF:			17. LIMITATION OF ABSTRACT	18. NUMBER OF PAGES	19a. NAME OF RESPONSIBLE PERSON
a. REPORT	b. ABSTRACT	c. THIS PAGE			
unclassified	**unclassified**	**unclassified**	**UU**	**8**	

multi-color operations are required. The handling of periodic structures that have slanted sidewalls often requires the artificial sectioning of such a layer into multiple sub-layers, which further increase the total number of layers that must be handled in modeling such structures. It is also well-known that many methods for imposing the required electromagnetic boundary conditions suffer increasing degree of instabilities with increasing number of layers.

Thirdly, realistic detectors often contain a multitude of different electromagnetic components. Other than the use of high and low dielectric materials mentioned above, the materials can be isotropic and biaxial electromagnetically, absorbing and non-absorbing, metallic and non-metallic, and form homogenous and periodic layers within the structure. Modeling of such devices therefore requires one to be able to handle successfully all these material components.

The electromagnetic properties of such a complex multilayered structure depend, sometimes sensitively, on a large number of material parameters such as the dielectric constants of the various components along different directions, and the widths and thicknesses of individual components within each layer. In detector design, this set of parameters must be optimized under a variety of constraints to achieve a certain performance goal. Modeling of photodetectors therefore requires the use of methods that are not only reliable, accurate and stable, but are highly efficient and have only modest memory requirements.

For this purpose, we have developed(Jiang et al. 2001) a modeling method based on the determination of the modal fields within each layer of the detector and then using them to represent the actual fields, and the use of the transmission-line technique to solve the resulting problem associated with the electromagnetic boundary conditions. Our method, referred to as the modal transmission-line (MTL) method, is fully capable of handling the stringent requirements mentioned above in connection with photodetector modeling.

In the MTL method, the modal fields within each of the periodic layer are computed from the eigenvalues and eigenvectors of a secular equation associated with Maxwell's equations. Our work here is to describe a method to transform such an equation into a form that can be solved very efficiently in the case of a normally incident wave. We then apply our method to illustrate how it can be used in modeling the C-QWIP mentioned above.

Throughout this paper, we assume that the incident field propagates perpendicularly to the structure, and that the entire structure can be decomposed into a multilayered one, where a common unit cell can be identified for all the periodic layers. This means that the periodicities of each of the periodic layers must be commensurate with each other. We further assume that within each periodic layer, the unit cell exhibits reflection symmetry about a constant-x plane passing through its center.

Symmetry is a familiar concept in the study of electron waves in crystalline materials and photonic bandgap crystals. Symmetries in electromagnetic waves are more interesting because other than the symmetries associated with the structure itself, there are internal symmetries due to Maxwell's equations themselves.

In the case of lamellar structures with a simple unit cell, the symmetry turns out to be rather simple, as we will discuss in this work. First we consider the case where the incident wave is symmetric just like the unit cell. An obvious example is the very common case of a normally incident plane wave. Owing to the symmetry of the unit cell, the modal fields in the structure can be classified as either symmetric or anti-symmetric. Since the incident fields are symmetric, they do not couple to the anti-symmetric modes at all. By explicitly eliminating such irrelevant modes in modeling symmetric structures within our modal-field representation of the scattering problem, we find that a numerical computational speedup of up to 8 times can be achieved. On the other hand, if the incident wave is anti-symmetric with respect to the symmetry plane, then only the anti-symmetric modal fields are coupled. An up to 8 times speedup can also be achieved.

Symmetrized modal fields can be employed as long as the incident wave falls normally onto the structure. Such an approach offers a significant numerical advantage even when the incident wave does not possess a definite symmetry. The reason is that a general normally incident wave can always be decomposed into a symmetric part and an anti-symmetric part. In addition, linear combinations of the Bloch plane waves (*i.e.* plane waves that obey Bloch's theorem) that exhibit symmetric and anti-symmetric properties can also be made. Owing to the linearity of the scattering problem, these two different types of waves can be dealt with separately using the present approach. A speedup of up to 4 times can still be achieved over the conventional approach which ignores symmetry considerations.

After deriving the resulting secular equations for the symmetric and anti-symmetric modes for the TE and TM cases, we apply our symmetrized modal field method to compute the scattering properties of the above C-QWIP structure. We also compare and contrast the results with those obtained from conventional modal-field method. First of all, we find that the numerical results for the eigenvalues and eigenvectors from two methods are practically identical within machine accuracy. The agreement in the final result for the absorption is better than 1×10^{-11}, but the results are obtained much quicker using the new method. The speedup factor indeed approaches closely the theoreti-

cal expected value of 8 as the number of harmonics included in the calculation is increased. Furthermore the present method reduces the required amount of memory by about one half.

2 SYMMETRIZED MODAL-FIELD METHOD

We are interested in a biaxial lamellar structure that is periodic along the x-direction. If a is the size of the primitive cell, then the reciprocal lattice vectors along the x-direction have magnitudes $K = 2\pi n/a$, where $n = 0, \pm 1, \ldots$. The basic structure of interest here is exactly the same as that studied in the past,(Tamir and Zhang 1996, Jiang, Tamir and Zhang 2001) except for the additional requirement that the structure must be symmetric about the center of each primitive cell. Thus if the origin in x is chosen to be at the center of one of the primitive cells, the dielectric constant satisfies

$$\epsilon^{\alpha}(-x) = \epsilon^{\alpha}(+x), \qquad \text{for } \alpha = x, y, z. \tag{1}$$

We therefore consider some general results for Fourier expansions and series that will be needed later. First any function $f(x)$ having the same periodicity as the lattice can be expanded as a Fourier series:

$$f(x) = \sum_{K} f_K \ \exp(iKx) \tag{2}$$

where the sum over K implies a sum over the integers that specify K, and the Fourier coefficients f_K are given by

$$f_K = \int_{-a/2}^{a/2} \frac{dx}{a} \ f(x) \ \exp(-iKx). \tag{3}$$

Alternatively $f(x)$ can be expressed in the form of a trigonometric Fourier series

$$f(x) = \tilde{f}_0 + \sum_{K>0} \left[\tilde{f}_K \ \cos(Kx) + \tilde{f}_{-K} \ \sin(Kx) \right]. \tag{4}$$

It is easy to see that these two sets of Fourier coefficients are related by

$$\tilde{f}_0 = f_0, \quad \tilde{f}_K = f_K + f_{-K}, \quad \tilde{f}_{-K} = i(f_K - f_{-K}). \tag{5}$$

The only restriction on $f(x)$ thus far is the periodic property.

Next if $f(x)$ is a symmetric function under reflection about the $x = 0$ plane, *i.e.* $f(-x) = f(x)$, so that $f(x)$ is an even function of x. In that case one can easily see from Eq. (3) that $f_{-K} = f_K$. Using this relation in Eq. (2) one finds that

$$f(x) \ = \ f_0 + 2 \sum_{K>0} f_K \ \cos(Kx). \tag{6}$$

Therefore one has

$$\tilde{f}_0 = f_0, \quad \tilde{f}_K = 2f_K, \quad \tilde{f}_{-K} = 0, \tag{7}$$

which can also be deduced from Eq. (5). For our calculation later, we find that it sometimes more convenient to rewrite the Fourier series expansion of a symmetric function $f(x)$ in the form

$$\begin{aligned} f(x) \ &= \ f_0 + \sum_{K>0} f_K \ \cos(Kx) + \sum_{K<0} f_{-K} \ \cos(Kx) \\ &= \ \sum_{K} f_K \ \cos(Kx), \end{aligned} \tag{8}$$

where the sum over K is unrestricted. We will next derive expressions for the modal fields. We find that it is more convenient to use Eq. (4) to express the modal fields, but Eq. (8) is better for the dielectric constants.

3 MODAL FIELDS

We consider here the modal fields inside a symmetric periodic layer located between $z = 0$ and t. The incident wave is assumed to be propagating along the z-direction, *i.e.* normal to the layer. We want to derive a secular equation that determines the modal fields within the periodic layer. The general fields are then expressed in terms of these modal fields.(Tamir and Zhang 1996, Jiang et al. 2001)

3.1 TE Mode

In the case of TE waves, the y-component of the electric field obeys the equation

$$[k_0^2 \epsilon^x(x) + \partial_x^2] E_y = -\partial_z^2 E_y. \tag{9}$$

In previous studies, E_y is expressed in terms of plane waves as

$$E_y = \sum_{K} \exp(iKx) \sum_{m} a_{K,m} v_m(z), \tag{10}$$

where

$$v_m(z) = f_m \exp(i\kappa_m z) + g_m \exp(i\kappa_m (t - z)) \tag{11}$$

are the equivalent voltages, m labels the modes, and the transverse component of the wavevector has been set to zero. It is known that the coefficients $a_{K,m}$ and κ_m are related to the eigenvectors and eigenvalues of the secular equation

$$\sum_{K'} [(K'^2 + \kappa_m^2)\delta_{K,K'} - k_0^2 \epsilon^x_{K-K'}] a_{K',m} = 0, \tag{12}$$

where $\delta_{K,K'}$ is the Kronnecker delta function. If a fixed integer N is chosen such that only the reciprocal lattice vectors between $-2\pi N/a$ and $2\pi N/a$ are retained in our calculation, then the secular equation becomes

an eigenvalue-eigenvector problem involving square matrices of size $(2N+1)$ by $(2N+1)$.

It is important to note that a symmetric wave, such as a plane wave, incident onto a symmetric structure can only couple to modes that are also symmetric. Therefore instead of using a Fourier series expansion of the fields, which exhibit no definite symmetry, it is better to use trigonometric Fourier series. Then we only need to include terms that are symmetric, *i.e.* the constant term and the cosine terms. Thus in Eq. (9) we let

$$E_y = \sum_{K\geq 0} \cos(Kx) \sum_m \tilde{a}_{K,m} v_m(z), \tag{13}$$

and use the cosine expansion of the form given in Eq. (8) for the dielectric function

$$\epsilon^x(x) = \sum_K \epsilon^x_K \ \cos(Kx). \tag{14}$$

Then we multiply the resulting equation by $\cos(Kx)$, with $K \geq 0$, and integrate within a unit cell to obtain the secular equation

$$\zeta_K (K^2 + \kappa_m^2)\tilde{a}_{K,m} - k_0^2 \sum_{K'\geq 0} \epsilon^+_{K,K'} \tilde{a}_{K',m} = 0. \tag{15}$$

where we define

$$\zeta_K = \begin{cases} 2, & \text{if } K = 0 \\ 1, & \text{otherwise} \end{cases} \tag{16}$$

and

$$\epsilon^+_{K,K'} = \epsilon_{K-K'} + \epsilon_{K+K'}. \tag{17}$$

If we keep only values of K between 0 and $2N\pi/a$, the above equation can be solved as a finite order matrix eigenproblem for the eigenvalues and eigenvectors, which yield κ_m^2 and $\tilde{a}_{K,m}$, respectively. There is a total of $N+1$ of these symmetric mode eigenvalue-eigenvectors pairs. They are part of the eigenvalue-eigenvectors pairs of the previous secular equation [Eq. (12)]. We have checked to verify that this is indeed so. Of course Eq. (8) also contains the eigenvalue-eigenvectors pairs of the anti-symmetric modes.

A secular equation for the anti-symmetric modes can be derived by expanding E_y in terms of only the sine function rather than the cosine function:

$$E_y = \sum_{K>0} \sin(Kx) \sum_m \tilde{a}_{-K,m} v_m(z). \tag{18}$$

Inserting Eq. (18) in Eq. (9), using the cosine expansion of the form given in Eq. (8) for the dielectric function, multiplying the resulting equation by $\sin(Kx)$ and integrating x over a unit cell, yields the secular equation for the anti-symmetric TE modes:

$$(K^2 + \kappa_m^2)\tilde{a}_{-K,m} - k_0^2 \sum_{K'>0} \epsilon^-_{K,K'} \tilde{a}_{-K',m} = 0. \tag{19}$$

In most practical situations, the incident field is itself symmetric with respect to the symmetry plane. A very common example is that of a plane incident wave. In that case, the anti-symmetric modes are not coupled at all to the incident wave, and therefore need not be computed. To obtain the modal fields within each of the periodic layers, all we need is to solve the secular equation for the symmetric modes using Eq. (15). By explicitly dealing with the relevant symmetric modes, we now only need to solve a $N+1$ by $N+1$ matrix instead of a $2N+1$ by $2N+1$ matrix for its eigenvalues and eigenvectors. Since the numerical complexity of matrix eigenproblem goes as the third power of the size of the matrix, we see that the computation should be about 8 times faster, since N is typically a large integer.

On the other hand, in the rare case where the incident field is anti-symmetric, then we need to solve the secular equation for the anti-symmetric modes using Eq. (19). We now only need to solve an N by N matrix instead of a $2N+1$ by $2N+1$ matrix for its eigenvalues and eigenvectors. Therefore we can also achieve a speed-up factor of about 8.

3.2 TM Mode

In the case of TM waves, the y-component of the magnetic field obeys the equation

$$[k_0^2 \epsilon^x(x) + \epsilon^x(x)\partial_x \eta^z(x) \partial_x] H_y = -\partial_z^2 H_y, \tag{20}$$

where $\eta^z(x) = 1/\epsilon^z(x)$. In previous studies, H_y is expressed in terms of plane waves as

$$H_y = \sum_K \exp(iKx) \sum_m b_{K,m} i_m(z), \tag{21}$$

where

$$i_m(z) = f_m \exp(i\kappa_m z) - g_m \exp(i\kappa_m (t-z)), \tag{22}$$

are equivalent currents. The coefficients $b_{K,m}$ and κ_m are related to the eigenvectors and eigenvalues of the secular equation

$$\sum_{K'} (k_0^2 \epsilon^x_{K-K'} - \kappa_m^2 \delta_{K,K'}) b_{K',m} \tag{23}$$
$$- \sum_{K'} \sum_{K"} \epsilon^x_{K-K'} K' \eta^z_{K'-K"} K" b_{K",m} = 0.$$

Equation (23) expresses a matrix eigenproblem for a $2N+1$ by $2N+1$ matrix if reciprocal lattice vectors between $-2\pi N/a$ and $2\pi N/a$ are retained.

It is known that (Li 1996) faster convergence is achieved if $\epsilon^x_{K-K'}$ is obtained by first inverting the matrix containing the Fourier coefficients of $1/\epsilon^x_{K-K'}$ and then taking the KK' element. Similarly $\eta^z_{K-K'}$ is obtained by first inverting the matrix containing the Fourier coefficients of $\epsilon^z_{K-K'}$ and then taking the KK' element.

We now derive the secular equation for symmetric TM modes in the trigonometric Fourier series representation by including in the expansion for the magnetic field only symmetric terms

$$H_y = \sum_{K\geq 0} \cos(Kx) \sum_m \tilde{b}_{K,m} i_m(z), \tag{24}$$

and use the cosine expansion of the form given in Eq. (8) for the dielectric function and an analogous one for $\eta^z(x)$

$$\eta^z(x) = \sum_K \eta^z_K \cos(Kx). \tag{25}$$

We use Eq. (24), Eq. (14), and Eq. (25) in Eq. (20), and then multiply the resulting equation by $\cos(Kx)$, with $K \geq 0$, and integrate within a unit cell. After some algebra we obtain the following secular equation for the symmetric TM modes

$$\sum_{K'\geq 0} (\zeta_K \kappa_m^2 \delta_{K,K'} - k_0^2 \epsilon^+_{K,K'}) \tilde{b}_{K',m} \tag{26}$$
$$+ \sum_{K'\geq 0} \sum_{K"\geq 0} \epsilon^+_{K,K'} K' \eta^-_{K',K"} K" \tilde{b}_{K",m} = 0.$$

This secular equation does not contain the unwanted anti-symmetric modes and as a result its eigenvalues and eigenvectors can be computed about 8 times faster than if one uses Eq. (23).

To find the secular equation for the anti-symmetric modes, we use the sine expansion for the magnetic field

$$H_y = \sum_{K>0} \sin(Kx) \sum_m \tilde{b}_{-K,m} i_m(z). \tag{27}$$

Using Eq. (27), Eq. (14), and Eq. (25) in Eq. (20), and multiplying the resulting equation by $\sin(Kx)$, with $K > 0$, and then integrating within a unit cell, we obtain the following secular equation for the anti-symmetric TM modes

$$\kappa_m^2 \tilde{b}_{-K,m} - k_0^2 \sum_{K'>0} \epsilon^-_{K,K'} \tilde{b}_{-K',m} \tag{28}$$
$$+ \sum_{K'>0} \sum_{K">0} \epsilon^-_{K,K'} K' \eta^+_{K',K"} K" \tilde{b}_{-K",m} = 0.$$

For a truncation value of N, this secular equation become an N by N matrix eigenproblem whose eigenvalues and eigenvectors determine the modal fields within such a periodic layer. In the case of an anti-symmetric incident wave, we can use this secular equation to find the modal fields about 8 times faster than using the conventional secular equation.

4 ALTERNATIVE DERIVATION

The above secular equations for the symmetric TE and TM modes can also be derived by considering the relations between the coefficients for the fields in the Fourier series representation with those in the trigonometric Fourier series representation. The general relation is given by Eq. (5). The derivation of the secular equations is more convenient if matrix notation is used.

For that purpose we define the following column vectors

$$\boldsymbol{f}_K = \begin{bmatrix} f_1 \\ f_2 \\ \vdots \end{bmatrix}, \quad \boldsymbol{f}_{-K} = \begin{bmatrix} f_{-1} \\ f_{-2} \\ \vdots \end{bmatrix}, \tag{29}$$

$$\tilde{\boldsymbol{f}}_K = \begin{bmatrix} \tilde{f}_1 \\ \tilde{f}_2 \\ \vdots \end{bmatrix}, \quad \tilde{\boldsymbol{f}}_{-K} = \begin{bmatrix} \tilde{f}_{-1} \\ \tilde{f}_{-2} \\ \vdots \end{bmatrix}. \tag{30}$$

We also define composite vectors

$$\bar{\boldsymbol{f}} = \begin{bmatrix} f_0 \\ \boldsymbol{f}_K \\ \boldsymbol{f}_{-K} \end{bmatrix}, \quad \tilde{\boldsymbol{f}} = \begin{bmatrix} \tilde{f}_0 \\ \tilde{\boldsymbol{f}}_K \\ \tilde{\boldsymbol{f}}_{-K} \end{bmatrix}, \tag{31}$$

and the transformation matrix

$$\boldsymbol{S} = \begin{bmatrix} 1 & 0 & 0 \\ 0 & \mathbf{1} & \mathbf{1} \\ 0 & i\mathbf{1} & -i\mathbf{1} \end{bmatrix}, \tag{32}$$

where $\mathbf{1}$ is an identity matrix. The relation given by Eq. (5) can then be expressed as

$$\tilde{\boldsymbol{f}} = \boldsymbol{S} \bar{\boldsymbol{f}}. \tag{33}$$

The inverse relation is given by

$$\bar{\boldsymbol{f}} = \boldsymbol{S}^{-1} \tilde{\boldsymbol{f}}, \tag{34}$$

where

$$\boldsymbol{S}^{-1} = \begin{bmatrix} 1 & 0 & 0 \\ 0 & \frac{1}{2}\mathbf{1} & -\frac{i}{2}\mathbf{1} \\ 0 & \frac{1}{2}\mathbf{1} & \frac{i}{2}\mathbf{1} \end{bmatrix}. \tag{35}$$

We define vectors $\boldsymbol{\epsilon}_K$ and $\boldsymbol{\epsilon}_{-K}$ analogous to Eq. (31), and a matrix $\boldsymbol{\epsilon}_{K,K}$ whose ij element is given by $\epsilon_{K_i - K_j}$.

4.1 TE Modes

We reconsider first the TE modes. In matrix notation we see that the secular equation in Eq. (12) in the usual plane wave basis can now be written as

$$(\bar{\boldsymbol{\epsilon}} - \bar{\boldsymbol{D}}) \bar{\boldsymbol{a}} = 0, \tag{36}$$

where we have defined

$$\bar{\boldsymbol{\epsilon}} = \begin{bmatrix} \epsilon_0 & \boldsymbol{\epsilon}^T_K & \boldsymbol{\epsilon}^T_{-K} \\ \boldsymbol{\epsilon}_K & \boldsymbol{\epsilon}_{K,K} & \boldsymbol{\epsilon}_{K,-K} \\ \boldsymbol{\epsilon}_{-K} & \boldsymbol{\epsilon}_{-K,K} & \boldsymbol{\epsilon}_{-K,-K} \end{bmatrix}, \tag{37}$$

$$\bar{\boldsymbol{D}} = \begin{bmatrix} \kappa^2 & \mathbf{0} & \mathbf{0} \\ \mathbf{0} & \boldsymbol{\Gamma} & \mathbf{0} \\ \mathbf{0} & \mathbf{0} & \boldsymbol{\Gamma} \end{bmatrix}, \tag{38}$$

$$\boldsymbol{\Gamma} = \boldsymbol{K}^2 + \kappa^2 \mathbf{1}, \tag{39}$$

where $\boldsymbol{K}$ is a diagonal matrix with diagonal elements $K_1, K_2, \ldots$, and the composite vector $\bar{\boldsymbol{a}}$ is defined as in Eq. (31). From Eqs. (34) one has $\bar{\boldsymbol{a}} = \boldsymbol{S}^{-1}\tilde{\boldsymbol{a}}$ and so we see that the secular equation in the trigonometric Fourier series basis is

$$(\tilde{\boldsymbol{\epsilon}} - \tilde{\boldsymbol{D}})\tilde{\boldsymbol{a}} = 0, \tag{40}$$

where for any $2N+1$ by $2N+1$ matrix $\boldsymbol{M}$, we define the matrix

$$\tilde{\boldsymbol{M}} = \boldsymbol{S}\bar{\boldsymbol{M}}\boldsymbol{S}^{-1}, \tag{41}$$

which is related to $\boldsymbol{M}$ by a similarity transformation.

One finds that $\tilde{\boldsymbol{D}} = \bar{\boldsymbol{D}}$ and

$$\tilde{\boldsymbol{\epsilon}} = \begin{bmatrix} \epsilon_0 & \boldsymbol{\epsilon}_K^T & \mathbf{0} \\ 2\boldsymbol{\epsilon}_K & \boldsymbol{\epsilon}_{K,K}^{+} & \mathbf{0} \\ \mathbf{0} & \mathbf{0} & \boldsymbol{\epsilon}_{K,K}^{-} \end{bmatrix}, \tag{42}$$

where we have defined

$$\boldsymbol{\epsilon}_{K,K}^{\pm} = \boldsymbol{\epsilon}_{K,K} \pm \boldsymbol{\epsilon}_{K,-K}. \tag{43}$$

Hence, we can prove that the secular equation for TE waves in the trigonometric Fourier series basis is given by

$$\begin{bmatrix} \epsilon_0 - \kappa^2 & \boldsymbol{\epsilon}_K^T & \mathbf{0} \\ 2\boldsymbol{\epsilon}_K & \boldsymbol{\epsilon}_{K,K}^{+} - \boldsymbol{\Gamma} & \mathbf{0} \\ \mathbf{0} & \mathbf{0} & \boldsymbol{\epsilon}_{K,K}^{-} - \boldsymbol{\Gamma} \end{bmatrix} \times \times \begin{bmatrix} \tilde{a}_0 \\ \tilde{\boldsymbol{a}}_K \\ \tilde{\boldsymbol{a}}_{-K} \end{bmatrix} = 0. \tag{44}$$

The eigenproblem is seen to decouple into two separate diagonal blocks. The first block, consisting of the first two equations, is for the symmetric modes. It is easy to see that they are equivalent to the secular equation that we derived earlier in Eq. (15).

The second block, consisting of the last equation, is clearly the secular equation for the anti-symmetric modes. This equation is in the form of an eigenproblem of an N by N matrix. If the incident wave is symmetric, these anti-symmetric modes cannot be excited and therefore there is no need to solve this secular equation at all. However if the incident wave is anti-symmetric, then we need to solve for the eigenvalues and eigenvectors of this secular equation, but not those for the symmetric modes. We also get a speed-up factor of up to 8 times compared with the conventional approach.

It is important to note that our approach of using symmetrized modal functions is applicable even when the incident wave has no definite symmetry. The reason is that a general incident wave can always be written as the sum of a symmetric part and an anti-symmetric part. Linearity of the electromagnetic problem implies that these two parts can be treated separately using their respective secular equations within the periodic layer. Consequently we expect to have a speed-up factor of up to 4 for high truncation value, N.

4.2 TM Modes

Next we reconsider the TM case using this matrix approach. The secular equation in the plane wave basis is given by Eq. (23), which can now be written in matrix notation as

$$\left(\bar{\boldsymbol{\epsilon}} - \kappa^2 \bar{\mathbf{1}} - \bar{\boldsymbol{\epsilon}}\bar{\boldsymbol{K}}\bar{\boldsymbol{\eta}}\bar{\boldsymbol{K}}\right)\bar{\boldsymbol{b}} = 0, \tag{45}$$

where $\bar{\mathbf{1}}$ is an identity matrix, and

$$\bar{\boldsymbol{\eta}} = \begin{bmatrix} \eta_0 & \boldsymbol{\eta}_K^T & \boldsymbol{\eta}_{-K}^T \\ \boldsymbol{\eta}_K & \boldsymbol{\eta}_{K,K} & \boldsymbol{\eta}_{K,-K} \\ \boldsymbol{\eta}_{-K} & \boldsymbol{\eta}_{-K,K} & \boldsymbol{\eta}_{-K,-K} \end{bmatrix}. \tag{46}$$

This equation can then be transformed into the trigonometric Fourier series basis by multiplying from the left by $\boldsymbol{S}$. The result is

$$\left(\tilde{\boldsymbol{\epsilon}} - \kappa^2 \tilde{\mathbf{1}} - \tilde{\boldsymbol{\epsilon}}\tilde{\boldsymbol{K}}\tilde{\boldsymbol{\eta}}\tilde{\boldsymbol{K}}\right)\tilde{\boldsymbol{b}} = 0, \tag{47}$$

where

$$\tilde{\mathbf{1}} = \bar{\mathbf{1}}, \tag{48}$$

and

$$\tilde{\boldsymbol{\eta}} = \begin{bmatrix} \eta_0 & \boldsymbol{\eta}_K^T & \mathbf{0} \\ 2\boldsymbol{\eta}_K & \boldsymbol{\eta}_{K,K}^{+} & \mathbf{0} \\ \mathbf{0} & \mathbf{0} & \boldsymbol{\eta}_{K,K}^{-} \end{bmatrix}, \tag{49}$$

with

$$\boldsymbol{\eta}_{K,K}^{\pm} = \boldsymbol{\eta}_{K,K} \pm \boldsymbol{\eta}_{K,-K}. \tag{50}$$

We can easily compute $\tilde{\boldsymbol{K}}$ and obtain from Eq. (47) the following secular equation for the TM modes in the trigonometric Fourier series basis

$$\left(\begin{bmatrix} \epsilon_0 & \boldsymbol{\epsilon}_K^T\boldsymbol{\Omega}^- & \mathbf{0} \\ 2\boldsymbol{\epsilon}_K & \boldsymbol{\epsilon}_{K,K}^{+}\boldsymbol{\Omega}^- & \mathbf{0} \\ \mathbf{0} & \mathbf{0} & \boldsymbol{\epsilon}_{K,K}^{-}\boldsymbol{\Omega}^+ \end{bmatrix} - \kappa^2 \boldsymbol{I}\right) \times \times \begin{bmatrix} \tilde{b}_0 \\ \tilde{\boldsymbol{b}}_K \\ \tilde{\boldsymbol{b}}_{-K} \end{bmatrix} = 0, \tag{51}$$

where

$$\boldsymbol{\Omega}^{\pm} = (\mathbf{1} - \boldsymbol{K}\boldsymbol{\eta}_{K,K}^{\pm}\boldsymbol{K}), \tag{52}$$

and

$$\boldsymbol{I} = \begin{bmatrix} 1 & \mathbf{0} & \mathbf{0} \\ \mathbf{0} & \mathbf{1} & \mathbf{0} \\ \mathbf{0} & \mathbf{0} & \mathbf{1} \end{bmatrix} \tag{53}$$

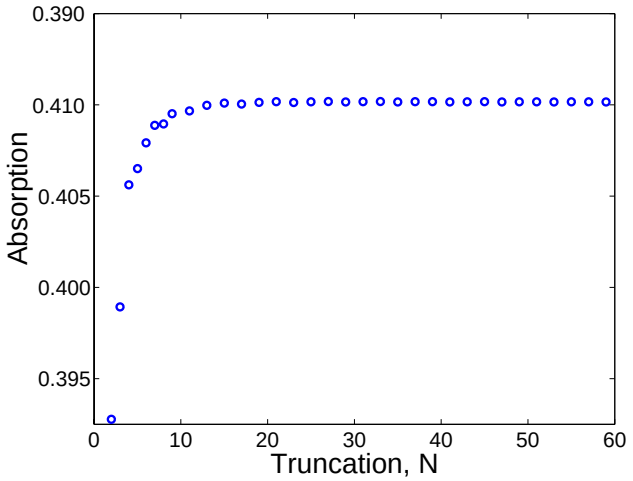

Figure 2: The absorption at a fixed wavelength (near the maximum) is plotted as a function of the truncation factor N.

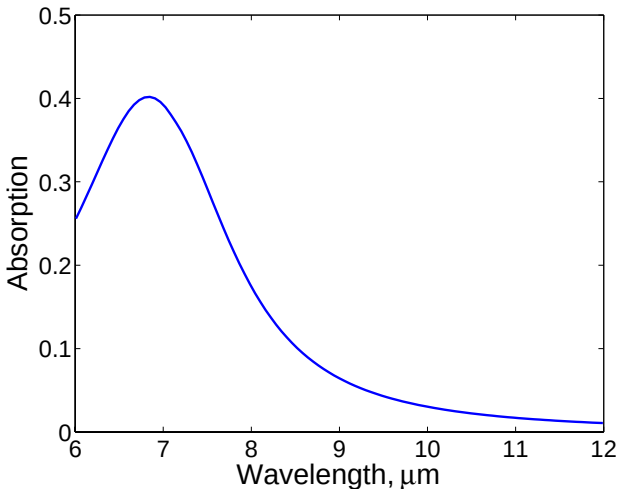

Figure 3: The absorption spectrum computed using a fixed value of the truncation factor N.

is the identity matrix. The matrix in Eq. (51) is seen to separate into two diagonal blocks. The first block, which consists of two parts, clearly determines the modes of the symmetric TM modes. The result can be seen to be equivalent to the secular equation that we derive earlier in Eq. (26). The second block on the other hand determines the modes of the anti-symmetric TM waves. These modes are not needed for symmetric normally incident waves.

Our alternate derivation of the secular equation clearly shows that both the symmetric and the anti-symmetric modes are contained in the conventional method that ignores symmetry considerations. The use of symmetrized modal field here enables one to ignore modes that do not have the right symmetry and are therefore irrelevant to the problem, and hence leads to in a more efficient numerical method.

5 RESULTS AND DISCUSSION

We will show the results of numerical computations of the scattering properties of a symmetric structure at normal incidence using the present method and compare them with those obtained using the conventional method. Our purpose here is to illustrate the superiority of the present method by considering as an example a practical C-QWIP structure, (Choi 1997, Mao et al. 2002, Choi et al. 2003, 2004a,b,c) as shown in Fig. 1.

First of all, we verify that the eigenvalues and eigenvectors obtained from the present method and the conventional method agree. Indeed we find that they are practically identical within machine accuracy. One of the most important quantity of interest in modeling QWIPs is the relative absorption, P_{abs} at any given wavelength. We find that using the resulting eigenvalues and eigenvectors to compute P_{abs}, the agreement is better than 1×10^{-11}.

Typically in our modeling work, the absorption spectrum is first computed using a moderate value of the truncation factor, N. To test for convergence of the results, we then fix the wavelength near one of the absorption peaks and repeat the computation of the spectrum using either methods for larger values of N. As a result we obtain a convergence curve as shown in Fig. 2. This curve provides us a good idea of the maximum error in the computed result at any given N. Using a value of N large enough to ensure that our results are accurate within a certain acceptable tolerance, we then recompute the spectrum. The result is shown in Fig. 3.

The above results were computed using the present symmetrized modal field method as well as the conventional method. Since they agree to better than 1×10^{-11} for any wavelength and truncation, the results from the above graphs will be practically identical. However the present method reduces the memory requirement to about one half that of the conventional method. It also runs much faster, as can be seen from Fig. 4, where the computation times for obtaining the absorption spectrum using these two methods are plotted as a function of N. We define a speed-up factor as the ratio of the computation time using the present method to that of the conventional method. The speed-up factor is shown in Fig. 5 as a function of N. We see that the speed-up factor increases with N and indeed gradually approaches the expected value of 8.

For the present somewhat simple C-QWIP, rather accurate absorption spectrum can be obtained in about 11.4 seconds for a given structure using a truncation value of $N = 15$. However in optimizing the performance of the detector, even if the material parameters are kept fixed, one still needs to explore numerous structures with layers having different widths, spacings

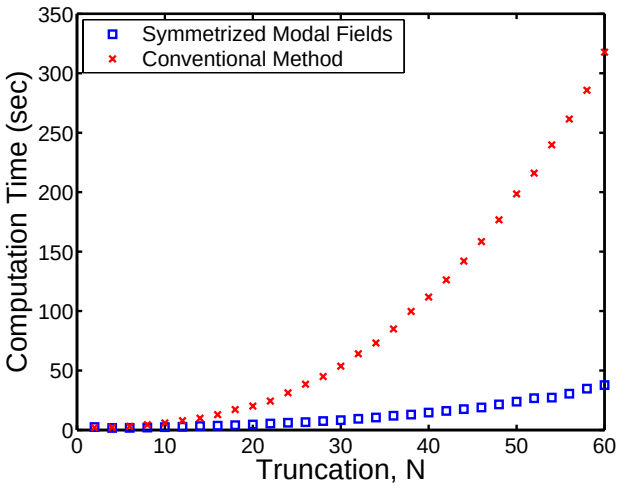

Figure 4: The total computation time for obtaining an absorption spectrum is plotted as a function of the truncation factor N.

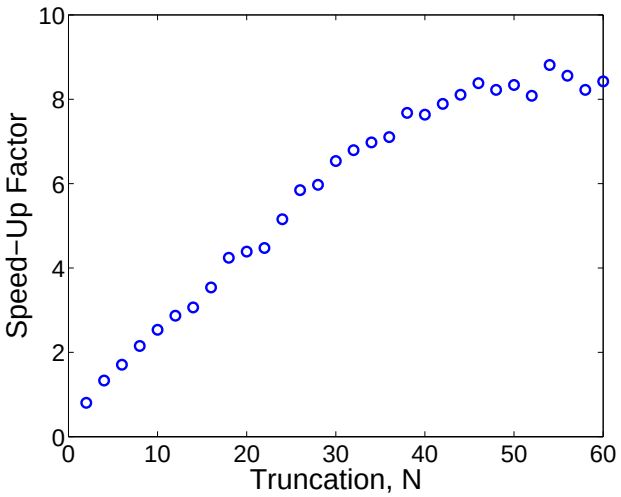

Figure 5: The speed-up factor as a function of the truncation factor N.

and thicknesses. For example if we want to vary only 4 out of the total of 6 dimensional parameters, and if each parameter can assume only 10 different values, then an exhaustive exploration of detector performance will take close to 32 hours using the conventional method. The speed-up factor for the new method at this truncation value is about 3.2. That means that the modeling can now be done in only about 10 hours. In general, the saving will be much greater for more complicated structures(Gunapala et al. 2000) and for higher accuracies.

ACKNOWLEDGMENTS

The authors wish to express their thanks to Drs. K. K. Choi (Army Research Laboratory), and S. Gunapala, S. Bandara (Jet Propulsion Laboratory) for valuable discussions on various aspects of QWIPs. In addition, thanks are also due to Dr. C. H. Lin for help with portions of this study. The present work was supported in part by the U.S. Army Research Office under Grant No. W911NF-04-1-0231.

REFERENCES

Choi, K. K., 1997: *The Physics of Quantum Well Infrared Photodetectors*. World Scientific.

Choi, K. K., Leung, K. M., Tamir, T. and Monroy, C., 2004a: Light Coupling Characteristics of Corrugated Quantum Well Infrared Photodetectors. *Appl. Phys. Letts.*, **84**, 4439–4441.

Choi, K. K., Leung, K. M., Tamir, T., Monroy, C., Wang, F. and Tsui, D. C., 2004b: Optimization of Corrugated QWIPs for High Speed Infrared Imaging. *to appear in SPIE*.

Choi, K. K., Lin, C. H., Leung, K. M., Tamir, T., Mao, J., Tsui, D. C. and Jhabvala, M., 2003: Broadband and Narrow Band Light Coupling for QWIPs. *Infrared Phys. and Tech.*, **44**, 309–324.

Choi, K. K., Monroy, C., Goldberg, A., Dang, G., Jhabvala, M., La, A., Tamir, T., Leung, K. M., Majumdar, A., Li, Jinjin and Tsui, D. C., 2004c: Designs and Applications of Corrugated QWIPs. *to appear in Infrared Phys. and Tech.*

Gunapala, S. D., Bandara, S. V., Singh, A., Liu, J. K., Rafol, S. B., Luong, E. M., Mumolo, J. M., Tran, N. Q., Ting, D. Z.-Y., Vincent, J. D., Shott, C. A., Long, J. and Levan, P. D., 2000: 640×486 Long-wavelength Two-color GaAs/AlGaAs Quantum Well Infrared Photodetector (QWIP) Focal Plane Array Camera. *IEEE Trans. Electr. Devices*, **47**, 963–971.

Jiang, M., Tamir, T. and Zhang, S., 2001: Modal Theory of Diffraction by Multilayered Gratings Containing Dielectric and Metallic Components. *J. Opt. Soc. Am. A*, **18**, 807–820.

Li, L., 1996: Use of Fourier Series in the Analysis of Discontinuous Periodic Structures. *J. Opt. Soc. Am. A*, **13**, 1870–1876.

Mao, J., Majumdar, A., Choi, K. K., Tsui, D. C., Leung, K. M., Lin, C. H., Tamir, T. and Vawter, G. A., 2002: Light Coupling Mechanism of Quantum Grid Infrared Photodetectors. *App. Phys. Letts.*, **80(3)**, 868–870.

Tamir, T. and Zhang, S., 1996: Modal Transmission-line Theory of Multilayered Grating Structures. *J. Lightwave Technol.*, **14**, 914–927.